Letter

Accurate reaction-diffusion limit to the spherical-symmetric Boltzmann equation

Shay I. Heizler,* Menahem Krief,* and Michael Assaf
Racah Institute of Physics, The Hebrew University, 9190401 Jerusalem, Israel

(Received 21 July 2023; accepted 28 December 2023; published 31 January 2024)

We resolve a long-standing question regarding the suitable effective diffusion coefficient of the spherical-symmetric transport equation, which is valid at long times. To that end, we generalize a transport solution in three dimensions for homogeneous media, to include general-collisional properties, including birth-death events and linearly anisotropic scattering. This is done by introducing an exact scaling law relating the Green's function of the pure-scattering case with the general-collision case, which is verified using deterministic and Monte Carlo simulations. Importantly, the effective diffusion coefficient is identified by inspecting the transport solution at long times.

DOI: 10.1103/PhysRevResearch.6.L012023

Introduction. The study of three-dimensional (3D) time-dependent transport phenomena is at the heart of many fields in physics, chemistry, and biology. For example, in astrophysics, when a massive star explodes, there is a blast of energy that is released in a relatively focused spot [1,2]. Similarly, in inertial confinement fusion a large focused release of energy occurs as a result of fusion reactions [3–5]. In these cases, x-ray photons are propagating fast toward the medium due to the radiative transfer mechanism. Correctly modeling the propagation of these heat waves is a prerequisite for analyzing the outgoing signals, e.g., from a supernova explosion. Time-dependent transport phenomena also appear in electron transport in hot plasmas [6], modeling coda waves of local earthquakes [7], the distribution of neutrons inside a nuclear reactor [8–10], and optical properties of biological tissues in biology [11–14]. Notably, in the latter, the balance between scattering and absorption inside the medium are of great interest [15]. Even in modeling the transport of bacteria that diffuse in a medium and may reproduce or die, a transport equation can be defined to model the population dynamics [16].

The exact particle propagation is modeled via the Boltzmann (transport) equation for the probability density function (PDF) $P(\vec{r},t,\hat{\Omega})$ per unit volume $d^3\vec{r}$ and direction $d\hat{\Omega}$, at time t. Notably, in most of the fields specified above, the governing equation of transport is of noninteracting particles, which are aptly described by the *linear* Boltzmann equation. When the medium is highly scattering, the exact solution of this equation includes a diffusive region in the bulk, and ballistic "tails" due to particles that almost do not undergo collisions [17–19]. However, obtaining the solution of the transport equation in the general case is not amenable analytically, and numerically it is highly time consuming. Notably, in a one-dimensional (1D) geometry, where the particles are free to travel only forward and backward, the linear transport equation reproduces the telegrapher's equation, which can be solved analytically [17,18,20–22].

It is well known that at sufficiently long times, the exact transport solution tends to a reaction-diffusion solution via the central limit theorem, due to multiple scattering events. The central part of the PDF has a Gaussian shape with increasing width, which corresponds to an effective diffusion coefficient. Naturally, applying a diffusion approximation to the transport equation gives rise to nonphysical tails of particles at $r > vt$ [23]. Yet, even in the bulk region where the diffusion approximation holds, it remains an open question of which diffusion coefficient to use to accurately reproduce the bulk solution of the full transport equation.

In some limits, e.g., in the purely scattering case, the effective diffusion coefficient is well known. The classic definition of the diffusion approximation uses the total mean free path (MFP), including absorption and scattering events [8,12,13,24,25]. On the other hand, some studies show that the diffusion coefficient should only depend on the scattering MFP [2,9,12,26–30]. When birth events are also included, a modified diffusion coefficient, accurate in the limit of source-dominant media, was offered in modeling the radiative transfer in astrophysics [2]. Yet, for an arbitrary collision scenario, or for highly anisotropic scattering, the corresponding effective diffusion coefficient is unknown [2,9,10,12–14,26–34].

Here, we present a simple yet rigorous derivation of the accurate diffusion coefficient, valid in the spherical-symmetric case, in the presence of an arbitrary set of processes, including birth (or branching) and death (or absorption) events, that may occur upon an interaction between an agent and the medium. This diffusion limit is crucial, e.g., in modeling radiative transfer in the non-LTE (local thermodynamic equilibrium) regime, when photon emission dominates absorption [2], which occurs in various astrophysical scenarios, such as

*These authors contributed equally to this work.

the shock breakout phase during supernovae, corona of accretion disks, and the nebular phase of stellar explosions, to name a few.

Our analysis is based on the generalization of the solution of Paasschens [18], which was obtained for a homogeneous infinite medium and pure isotropic scattering. While in Ref. [35] the solution was extended to the case of linear anisotropic scattering, we here generalize the solution to hold for an arbitrary collision scenario. We first derive an exact scaling relation (in space and time) of the 3D transport solution between the pure-scattering and general-collision case, which holds for the general anisotropic case as well, and find the Green's function solution for a point source term. The scaling relation is verified via two different numerical schemes: (i) a solution of the deterministic time-dependent equation with the discrete ordinate method (S_N method) [36], and (ii) stochastic Monte Carlo (MC) simulations mimicking the different probabilistic events [see Supplemental Material (SM) Sec. I [37]]. This scaling relation allows us to extend the analytical solution of Paasschens for the general-collision case, from which we infer the diffusion coefficient by computing its long-time asymptotics.

Spherical-symmetric transport solution. In the case of no external forces and assuming monoenergetic particles, the governing equation is the *linear* Boltzmann transport equation. For a spherical-symmetric setting, the transport equation takes the following form [8,18,25,36] (see SM Sec. II and Sec. III [37]):

$$\left(\frac{\partial}{v\partial t}+\mu\frac{\partial}{\partial r}+\frac{1-\mu^2}{r}\frac{\partial}{\partial\mu}+\ell_t^{-1}\right)P(r,t,\mu) = \frac{c(r,t)\ell_t^{-1}}{2}\int_{-1}^{1}d\mu f(\mu_0)P(r,t,\mu)+Q_{\rm ext}(r,t,\mu)/v. \tag{1}$$

Here, the PDF, $P(r,t,\mu)$, is a function of the radius r, time t, and the direction of the particle with respect to r, $\mu\equiv\hat{\Omega}\cdot\hat{r}$, where $\hat{\Omega}$ is the direction of the particle before the collision. In addition, we have assumed that the interaction between particles is negligible, and the medium is locally in equilibrium, such that the Boltzmann collision term can be modeled using the definitions of the MFPs (or cross sections) for different interactions. These are the MFPs of absorption, ℓ_a, and of scattering, ℓ_s, where we denote by ℓ_t the total MFP due to all physical events. In general, the scattering event is a function of the angular deflection during scattering, i.e., the angle between the direction of the particle before the scattering $\hat{\Omega}$ and after $\hat{\Omega}'$ [38]. As a result, the *macroscopic cross section* for scattering has the form $\Sigma_s(\hat{\Omega}\to\hat{\Omega}')=\ell_s^{-1}f(\hat{\Omega}\cdot\hat{\Omega}')=\ell_s^{-1}f(\mu_0)$, where $f(\mu_0)$ is a normalized distribution of the deflection angle cosine $\mu_0\equiv\hat{\Omega}\cdot\hat{\Omega}'$. The function f is problem dependent, and is commonly taken in the Henyey-Greenstein form [39] (see SM Sec. IVa [37]) [40]. Therefore, the collision term in Eq. (1) can be written explicitly as a "gain-loss" term using the above MFP definitions.

Additional notations in Eq. (1) include the particle velocity v and an external source $Q_{\rm ext}(r,t,\mu)$, which may be a function of space, direction, and time. Finally, $c(r,t)$ represents the mean number of particles that are emitted in an interaction, including sources [8–10,23–25,41–44], for example, due to cell division, and satisfies [45]

$$c(r,t)=\frac{\ell_s^{-1}\mathcal{P}(r,t)+\frac{1}{2}\int_{-1}^{1}Q_{\rm int}(r,t,\mu)d\mu/v}{\ell_t^{-1}\mathcal{P}(r,t)}. \tag{2}$$

Here, $\mathcal{P}(r,t)=\frac{1}{2}\int_{-1}^{1}d\mu P(r,t,\mu)$ is the population probability density, which depends only on the magnitude of r and time. In the case of no internal source and homogeneous media, $0\leqslant c\leqslant 1$ becomes the ratio of the total and scattering MFPs, $c=\ell_s^{-1}/\ell_t^{-1}=\ell_s^{-1}/(\ell_s^{-1}+\ell_a^{-1})$. If the medium involves internal sources such as birth events proportional to $\mathcal{P}(\vec{r},t)$, one has $c=(\ell_s^{-1}+\bar{n}\ell_b^{-1})/\ell_t^{-1}=(\ell_s^{-1}+\bar{n}\ell_b^{-1})/(\ell_s^{-1}+\ell_a^{-1}+\ell_b^{-1})$ which may exceed 1. Here, $\bar{n}$ is the mean number of particles created in a birth event and ℓ_b is the birth MFP. Clearly, in systems with $c<1$ ($c>1$) the expected number of particles decays (exponentially grows) in time. For example, in astrophysics, the emitted blackbody energy density B and radiation energy density E allow us to define c as $c\equiv\omega_{\rm eff}=(\ell_a^{-1}B+\ell_s^{-1}E)/\ell_t^{-1}E$. While in LTE, $E\approx B$ and thus $\omega_{\rm eff}\approx 1$, in non-LTE, when the matter is hotter than the radiation, $B>E$ and $\omega_{\rm eff}>1$, and vice versa [2]. Naturally, when $c>1$, the exponential growth is eventually arrested by nonlinear effects.

Henceforth, we focus on the case of infinite homogeneous medium, i.e., we assume $c(r,t)=c$ is a constant. Importantly, we perform our calculations below using an external pointlike source at the origin, $Q_{\rm ext}(r,t)=\delta(r)\delta(t)/4\pi r^2$, where $\delta(x)$ is the Dirac delta function. In this case, the calculated population density will serve as the Green's function, which will allow the subsequent calculation of the population density for any space- and time-dependent external source term by the Green's convolution integral.

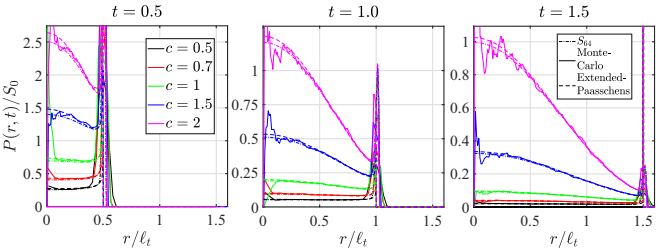

FIG. 1. The population density $\mathcal{P}(r,t)$ at different times for various values of c [Eq. (2)] (see legend) in the isotropic case. Our analytical solution, Eq. (5) (dashed lines), is compared with the numerical solution using the S_N (dashed-dotted lines) and MC (solid lines) methods. The noisy solution at $r\simeq 0$ is due to the small volumes of the numeric cells near the origin.

In Fig. 1 we compare our analytical solution to Eq. (1) [given by Eq. (5) below] to numerical solutions using the S_N and MC methods. Here, we show $\mathcal{P}(r,t)$ as a function of the rescaled position $\tilde{r}=r/\ell_t$, at different rescaled times $\tilde{t}=tv/\ell_t$, for various values of c, $0.5\leqslant c\leqslant 2$. Both the analytical and numerical solutions show ballistic behavior near $r=vt$. Yet, the ballistic region shrinks and the diffusive behavior becomes dominant as time advances.

We now solve Eq. (1) in the general-collision scenario, i.e., $c\neq 1$. To do so, we identify a scaling relation between the PDF, $P(r,t,\mu;c)$, in the general $c\neq 1$ case, and the PDF,

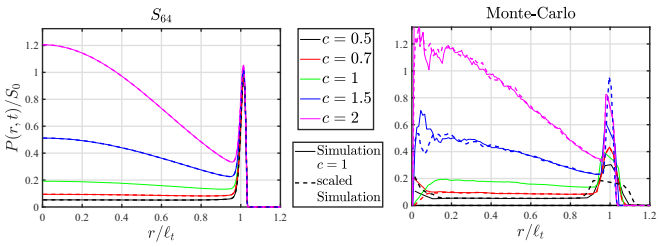

FIG. 2. A numerical verification of the scaling relation [Eq. (3)] for various values of c. The solid lines represent the S_N (left) and MC (right) results for the population densities, calculated with a specific value of c, while the dashed lines are the rescaled results with $c = 1$, using Eq. (3).

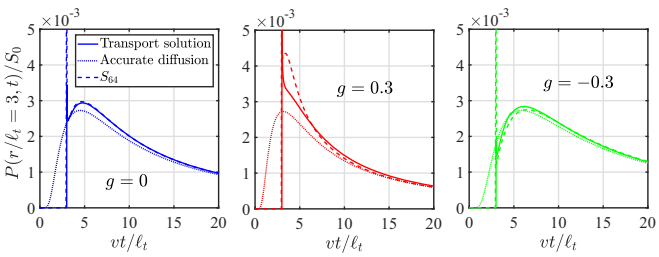

FIG. 3. The population density $\mathcal{P}(r,t)$ vs the normalized time vt/ℓ, at $\tilde{r} = 3$ (right), for various values of anisotropy g. Shown are the results obtained from the extended Paasschens solution (solid lines), S_N simulations (dashed lines), and the accurate diffusion equation, see [9] (dotted lines).

$P(r,t,\mu;1)$, in the pure-scattering, $c = 1$, case. Previously, it was shown that for $c \leqslant 1$, the scaling relation reads [18,30,35] $P(r,t,\mu;c) = e^{-vt/\ell_a} P(r,t,\mu;1)$, with $c = \ell_s^{-1}/(\ell_a^{-1} + \ell_s^{-1})$. We propose the following exact scaling relation for the Boltzmann equation in spherical symmetry (1), for a general value of c (see SM Sec. III [37]),

$$P(r,t,\mu;c) = c^3 e^{-(1-c)vt/\ell_t} P(cr, ct, \mu; 1), \tag{3}$$

where ℓ_t denotes the total MFP. In Fig. 2 we numerically verify the scaling relation by plotting $\mathcal{P}(r,t)$ using the S_N and MC methods, for various values of c, both in the ballistic and diffusion regions.

We now use this scaling relation to find the solution for the population density $\mathcal{P}(r,t;c)$, for $c \neq 1$. Here, our starting point is the result in the pure-scattering case, $c = 1$, obtained by Paasschens [18]. This result assumes a homogeneous infinite medium, and was obtained exactly for 2D and 4D geometries using a Fourier transform in space and time. Interestingly, this method is less useful in the 3D case as the inverse transform cannot be found analytically. Instead, Paasschens used an interpolation between the 2D and 4D solutions [18], which yields $\mathcal{P}(r,t;1)$ in the 3D case,

$$\begin{aligned}\mathcal{P}(r,t;1) \simeq{}& \frac{e^{-vt/\ell_s}}{4\pi r^2}\delta(r-vt) + \frac{(1-r^2/v^2t^2)^{1/8}}{(4\pi\ell_s vt/3)^{3/2}} e^{-vt/\ell_s} \\ &\times G\left(\frac{vt}{\ell_s}\left[1-\frac{r^2}{v^2t^2}\right]^{3/4}\right)\Theta(vt-r), \\ G(x) ={}& 8(3x)^{-3/2}\sum_{N=1}^{\infty}\frac{\Gamma\left(\frac{3}{4}N+\frac{3}{2}\right)}{\Gamma\left(\frac{3}{4}N\right)}\frac{x^N}{N!},\end{aligned} \tag{4}$$

where $\Theta(r)$ is the Heaviside step function and $\Gamma(x)$ is the gamma function. Notably (see below), at long times Eq. (4) converges to the diffusion solution with $D = v\ell_t/3$ and $c = 1$. Solution (4) can be extended to the linear anisotropic scattering case, upon using $\ell_{\rm tr}$ instead of ℓ_t, where $\ell_{\rm tr}^{-1} \equiv \ell_t^{-1}(1-g)$, and $g = \bar{\mu}_0$ denotes the average scattering angle cosine [35]. Here, $\ell_{\rm tr}$ is called the *transport MFP* [25]. However, we show that this solution is valid only at long times (see SM Sec. IVa [37]).

With the scaling relation (3) we have found, and using Eq. (4) for $c = 1$, the general solution for the population density, $\mathcal{P}(r,t;c)$ for $c \neq 1$ reads (see SM Sec. IVb [37])

$$\begin{aligned}\mathcal{P}(r,t;c) \simeq{}& \frac{e^{-vt(1-cg)/\ell_t}}{4\pi r^2}\delta(r-vt) + \frac{(1-r^2/v^2t^2)^{1/8}}{\{4\pi\ell_t vt/[3c(1-g)]\}^{3/2}} \\ &\times G\left(\frac{vct(1-g)}{\ell_t}\left[1-\frac{r^2}{v^2t^2}\right]^{3/4}\right) \\ &\times e^{-vt(1-cg)/\ell_t}\Theta(vt-r).\end{aligned} \tag{5}$$

This solution coincides with the Paasschens solution for $c = 1$ and $g = 0$. It can be shown to be valid for $g \ll 1$ at all times; yet, it becomes valid for all values of g, $-1 < g < 1$, at long times (see SM Sec. IV [37]).

In Fig. 1 our analytical solution [Eq. (5)] is shown to excellently agree with the numerical results of both S_N and MC, for all values of c, in the isotropic case. In Fig. 3 we test the accuracy of Eq. (5) for the general anisotropic case for $c = 1$. Here, we plot the PDF for the dimensionless spatial position $\tilde{r} = 3$, as a function of $\tilde{t}$ for isotropic ($g = 0$), forward ($g = 0.3$), and backward ($g = -0.3$) scattering. Importantly, we have checked that our results exactly reproduce earlier benchmark results for these g values [9]. While for $g = 0$ our solution coincides with Eq. (4), and is thus accurate at all times, for $g \neq 0$ the picture is different. For forward scattering ($g = 0.3$) Eq. (5) yields a good agreement only at late times, whereas for backward scattering ($g = -0.3$), Eq. (5) yields a good agreement also for earlier times (see Fig. 3). This is because forward scattering increases anisotropy, thereby delaying the validity of the diffusion assumption. Conversely, backward scattering causes particles to return to the origin, thereby increasing isotropy. It is also demonstrated that for the various values of g, the diffusion approximation yields solutions that propagate faster than the particle speed at early times, and converge to the exact solution at long times.

Determining the diffusion coefficient at long times. We now identify the effective diffusion coefficient by computing the late-time asymptotics of Eq. (1). At late times, $t \gg v/\ell_t$, the PDF is close to being isotropic and we can use the so-called *diffusion assumption*, $P(r,t,\mu) \approx \mathcal{P}(r,t) + 3\mu\mathcal{P}_1(r,t)$, with $\mathcal{P}_1(r,t) \equiv \int_{-1}^{1} \mu d\mu P(r,t,\mu)$ being the flux. Integrating Eq. (1) once over $\int d\mu$ and once over $\int \mu d\mu$

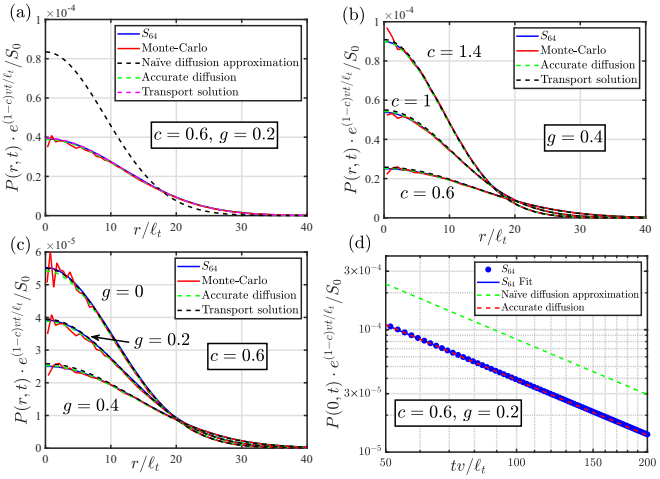

FIG. 4. (a) The population density $\mathcal{P}(r,t)$ at long times ($vt/\ell = 100$), for $c = 0.6$ and $g = 0.2$, vs the normalized space coordinate vt/ℓ. Shown are the full transport solutions obtained from the S_N method (blue curves), MC simulations (red curves), and the full analytical solution (5) (magenta), which are compared with the results of the naive diffusion approximation (black) and the accurate diffusion approximation (8) (green curves). (b) The population density $\mathcal{P}(r,t)$ at long times ($vt/\ell = 100$), for different values of c ($g = 0.2$), exact (S_N, MC, and analytic) vs the accurate diffusion solution. (c) Same as in (b) for different values of g ($c = 0.6$). (d) A log-log plot of the population density at the origin $\mathcal{P}(0,t)$, for $c = 0.6$ and $g = 0.2$, as a function of the normalized time vt/ℓ. Here, results of the naive (green) and accurate (red) diffusion solutions are compared with the S_N solution (blue).

yields two equations for the zeroth and first moments of the PDF. After some algebra we obtain

$$\frac{\partial \mathcal{P}(r,t)}{v\partial t} + \frac{1}{r^2}\frac{\partial}{\partial r}[r^2\mathcal{P}_1(r,t)] + \frac{1-c}{\ell_t}\mathcal{P}(r,t) = \frac{Q_{\rm ext}(r,t)}{v}, \tag{6a}$$

$$\mathcal{P}_1(r,t) = -\frac{\ell_t}{3(1-g)}\frac{\partial \mathcal{P}(r,t)}{\partial r} = -\frac{D_{\rm tr}}{v}\frac{\partial \mathcal{P}(r,t)}{\partial r}. \tag{6b}$$

Note that while Eq. (6a) is exact, Eq. (6b) is an approximated Fick's law, using the diffusion assumption, and neglecting the $\partial\mathcal{P}_1(r,t)/\partial t$ term compared to $(v/\ell_t)\mathcal{P}_1(t,r)$ [46]. Substituting Eq. (6b) in Eq. (6a) yields a *reaction-diffusion* equation [47,48], with a diffusion constant of $D_{\rm tr} \equiv v\ell_{\rm tr}/3$, where $\ell_{\rm tr}$ was defined above [8,12,13,24,25]. The solution of Eqs. (6) yields

$$\mathcal{P}_{\rm diff}(r,t;c) = \frac{1}{(4\pi D_{\rm tr}t)^{3/2}}\exp\left[-\frac{r^2}{4D_{\rm tr}t} - \frac{vt(1-c)}{\ell_t}\right]. \tag{7}$$

Yet, this solution yields an incorrect scaling relation $\mathcal{P}_{\rm diff}(r,t;c) = \mathcal{P}_{\rm diff}(r,t;1)e^{-(1-c)vt/\ell_t}$ and thus violates the scaling in Eq. (3) for $c \neq 1$ [12,13]. This is also evident by comparing Eq. (7) to numerical results, revealing that the approximation given by the first two moments leading to Eqs. (6) breaks down at $c \neq 1$ (see Fig. 4).

To find the correct diffusion coefficient for any $c \neq 1$, we use Eq. (5) in the limit of $t \to \infty$, which reads

$$\mathcal{P}(r, t\to\infty; c) = \frac{1}{\left(4\pi\frac{D_{\rm tr}}{c}t\right)^{3/2}}\exp\left[-\frac{r^2}{4\frac{D_{\rm tr}}{c}t} - \frac{vt(1-c)}{\ell_t}\right]. \tag{8}$$

This solution coincides with the diffusion solution (7), but with a *modified* diffusion coefficient, $D'_{\rm tr} \equiv D_{\rm tr}/c = v\ell_{\rm tr}/(3c)$, which is exact, even when the classical diffusion assumption is invalid. This result can also be obtained directly by applying the scaling relation to Eq. (7) for $c = 1$: $\mathcal{P}_{\rm diff}(cr, ct; c) = c^3 e^{-(1-c)vt/\ell_{\rm tr}}\mathcal{P}_{\rm diff}(cr, ct; 1)$. Notably, while our result holds for any value of c, in the special case of $c \leqslant 1$, the diffusion constant becomes $D = v\ell_s/3$, and provides a rigorous basis for previous semiempirical studies that obtained a similar result [2,9,12,26–30]. Finally, one can also derive a diffusion equation directly from the transport equation (1) at $t \to \infty$, without explicitly assuming the diffusion assumption, which yields the correct diffusion coefficient in the close vicinity of $c \simeq 1$ (see SM Sec. V [37]).

In Figs. 4(a)–4(c) we compare the probability density $\mathcal{P}(r,t;c)$ given by Eq. (8) as a function of r, with numerical solutions of Eq. (1) at late times, using the S_N and MC methods, for different values of g and c. The figure shows that the naive choice of $D = v\ell_t/3$ yields large errors. On the other hand, using the accurate diffusion constant $D = v\ell_t/[3c(1-g)]$ yields an excellent agreement, indicating that the proposed general-collision diffusion coefficient accurately reproduces the solution to the transport equation [Eq. (5)] at late times, for any c or g.

A complementary view to the spatial profiles is to use the value at the center of the Gaussian, $\mathcal{P}(0, t\to\infty)$ as a function of time [as can be seen from Eqs. (7) and (8)], which can be numerically found by fitting the S_N solution. In Fig. 4(d) we plot $\mathcal{P}(0,t)e^{(1-c)vt/\ell_t}$ and compare the different diffusion coefficients from Fig. 4(a). Again, using $D = v\ell_{\rm tr}/(3c)$ yields an excellent agreement with the S_N results. However, the naive choice of $D = v\ell_t/3$ yields a highly inaccurate result.

Discussion. A long-standing question in the field of statistical physics, is the identification of the diffusion coefficient in the diffusion limit of the 3D transport equation, for an arbitrary set of reactions, i.e., $c \neq 1$, and weakly anisotropic scattering. Here, we identify the correct diffusion coefficient by deriving a generalized solution for the point source Green's function for the 3D spherical-symmetric transport equation. This was done by introducing an exact scaling relation between the general-collision ($c \neq 1$) and pure-scattering ($c = 1$) solutions. We verified our analytical results using the S_N method and Monte Carlo simulations. Unlike previous results [2,9,12,26–30], the diffusion coefficient we have derived is accurate for any c, i.e., for arbitrary birth-death reactions. These results may provide important insight into fields such as photon diffusion in tissue optics and radiative transfer in nonequilibrium astrophysics.

Acknowledgment. M.A. acknowledges support from the Israel Science Foundation Grant No. 531/20.

[1] J. I. Castor, *Radiation Hydrodynamics* (Cambridge University Press, Cambridge, UK, 2004).

[2] C. Levermore and G. Pomraning, A flux-limited diffusion theory, Astrophys. J. **248**, 321 (1981).

[3] H. Abu-Shawareb *et al.* (Indirect Drive ICF Collaboration), Lawson criterion for ignition exceeded in an inertial fusion experiment, Phys. Rev. Lett. **129**, 075001 (2022).

[4] A. B. Zylstra, A. L. Kritcher, O. A. Hurricane, D. A. Callahan, K. Baker, T. Braun, D. T. Casey, D. Clark, K. Clark, T. Döppner *et al.*, Record energetics for an inertial fusion implosion at NIF, Phys. Rev. Lett. **126**, 025001 (2021).

[5] J. D. Lindl, P. Amendt, R. L. Berger, S. G. Glendinning, S. H. Glenzer, S. W. Haan, R. L. Kauffman, O. L. Landen, and L. J. Suter, The physics basis for ignition using indirect-drive targets on the national ignition facility, Phys. Plas. **11**, 339 (2004).

[6] L. Spitzer and R. Härm, Transport phenomena in a completely ionized gas, Phys. Rev. **89**, 977 (1953).

[7] E. Carcolé and A. Ugalde, Formulation of the multiple anisotropic scattering process in two dimensions for anisotropic source radiation, Geophys. J. Int. **174**, 1037 (2008).

[8] K. Case and P. Zweifel, *Linear Transport Theory* (Addison-Wesley, Reading, MA, 1967).

[9] B. Ganapol, Reconstruction of the time-dependent monoenergetic neutron flux from moments, J. Comput. Phys. **59**, 468 (1985).

[10] S. Dulla, S. Canepa, and P. Ravetto, From transport to diffusion through a space asymptotic approach, Math. Comput. Simul. **80**, 2134 (2010).

[11] H. C. van de Hulst and R. Graaff, Aspects of similarity in tissue optics with strong forward scattering, Phys. Med. Biol. **41**, 2519 (1996).

[12] T. Durduran, A. G. Yodh, B. Chance, and D. A. Boas, Does the photon-diffusion coefficient depend on absorption? J. Opt. Soc. Am. A **14**, 3358 (1997).

[13] R. Aronson and N. Corngold, Photon diffusion coefficient in an absorbing medium, J. Opt. Soc. Am. A **16**, 1066 (1999).

[14] R. Graaff and J. J. T. Bosch, Diffusion coefficient in photon diffusion theory, Opt. Lett. **25**, 43 (2000).

[15] R. Graaff and B. J. Hoenders, *Telegrapher's Equation for Light Transport in Tissue with Substantial Absorption, Biomedical Optics*, OSA Technical Digest (CD) (Optica Publishing Group, Washington, DC, 2008), paper BSuE52.

[16] H. G. Othmer and T. Hillen, The diffusion limit of transport equations derived from velocity-jump processes, SIAM J. Appl. Math. **61**, 751 (2000).

[17] R. Metzler and J. Klafter, The random walk's guide to anomalous diffusion: A fractional dynamics approach, Phys. Rep. **339**, 1 (2000).

[18] J. C. J. Paasschens, Solution of the time-dependent Boltzmann equation, Phys. Rev. E **56**, 1135 (1997).

[19] E. Barkai and S. Burov, Packets of diffusing particles exhibit universal exponential tails, Phys. Rev. Lett. **124**, 060603 (2020).

[20] S. Goldstein, On diffusion by discontinuous movements, and on the telegraph equation, Q. J. Mech. Appl. Math. **4**, 129 (1951).

[21] G. H. Weiss, Some applications of persistent random walks and the telegrapher's equation, Physica A **311**, 381 (2002).

[22] J. M. Porrà, J. Masoliver, and G. H. Weiss, When the telegrapher's equation furnishes a better approximation to the transport equation than the diffusion approximation, Phys. Rev. E **55**, 7771 (1997).

[23] S. I. Heizler, Asymptotic telegrapher's equation (P_1) approximation for the transport equation, Nucl. Sci. Eng. **166**, 17 (2000).

[24] K. Case, F. Hoffmann, and G. Placzek, *Introduction to the Theory of Neutron Diffusion*, Vol. I (Los Alamos Scientific Laboratory, NM, 1953).

[25] G. I. Bell and S. Glasstone, *Nuclear Reactor Theory* (Van Nostrand Reinhold. New York, 1970).

[26] K. Furutsu and S. Ito, Diffusion equation derived from the space-time transport equation and light pulse propagation through thick clouds, Radio Sci. **16**, 1201 (1981).

[27] G. Pomraning, A comparison of various flux limiters and Eddington factors, Lawrence Livermore National Laboratory Report No. UCID-19220 (1981).

[28] K. Furutsu and Y. Yamada, Diffusion approximation for a dissipative random medium and the applications, Phys. Rev. E **50**, 3634 (1994).

[29] Y. Tsuchiya and T. Urakami, Photon migration model for turbid biological medium having various shapes, Jpn. J. Appl. Phys. **34**, L79 (1995).

[30] A. Zoia, E. Dumonteil, and A. Mazzolo, Collision densities and mean residence times for d-dimensional exponential flights, Phys. Rev. E **83**, 041137 (2011).

[31] R. Graaff and B. J. Hoenders, Diffusion theory for light propagation in biological tissue: limitations and adaptations, in *Saratov Fall Meeting 2004: Optical Technologies in Biophysics and Medicine VI*, Vol. 5771, edited by V. V. Tuchin, International Society for Optics and Photonics (SPIE, Bellingham, WA, 2005), pp. 28–41.

[32] B. J. Hoenders and R. Graaff, Telegrapher's equation for light derived from the transport equation, Opt. Commun. **255**, 184 (2005).

[33] A. Liemert and A. Kienle, Analytical solution of the radiative transfer equation for infinite-space fluence, Phys. Rev. A **83**, 015804 (2011).

[34] A. Liemert and A. Kienle, Infinite space Green's function of the time-dependent radiative transfer equation, Biomed. Opt. Express **3**, 543 (2012).

[35] F. Martelli, A. Sassaroli, A. Pifferi, A. Torricelli, L. Spinelli, and G. Zaccanti, Heuristic Green's function of the time dependent radiative transfer equation for a semi-infinite medium, Opt. Express **15**, 18168 (2007).

[36] E. E. Lewis and W. F. Miller, *Computational Methods of Neutron Transport* (American Nuclear Society, Downers Grove, IL, 1993).

[37] See Supplemental Material at http://link.aps.org/supplemental/10.1103/PhysRevResearch.6.L012023 for more details on the derivations and additional results from the analysis and simulations.

[38] Note that in this spherical-symmetric case, the particle changes its direction μ even by undergoing a pure ballistic motion from $\vec{r}_1$ to $\vec{r}_2$.

[39] L. Henyey and J. Greenstein, Diffuse radiation in the galaxy, Astrophys. J. **93**, 70 (1941).

[40] Here, the function f is taken to be of the form $f(\mu_0) = (1/2)(1-g^2)/(1+g^2-2g\mu_0)^{3/2}$, where $g = \bar{\mu}_0$ denotes the average scattering angle cosine [35].

[41] I. Kuščer and P. F. Zweifel, Time-dependent one-speed albedo problem for a semi-infinite medium, J. Math. Phys. **6**, 1125 (1965).

[42] R. J. Doyas and B. L. Koponen, Linearly anisotropic extensions of asymptotic neutron diffusion theory, Nucl. Sci. Eng. **41**, 226 (1970).

[43] A. M. Winslow, Extensions of asymptotic neutron diffusion theory, Nucl. Sci. Eng. **32**, 101 (1968).

[44] E. d'Eon, *A Hitchhiker's Guide to Multiple Scattering, Exact Analytic, Monte Carlo and Approximate Solutions in Transport Theory* (eugenedeon.com/hitchhikers, 2022).

[45] Here, c is often called ω_{eff} in radiative transfer [2,27] and a in optics [11,14,15,31,32].

[46] Without neglecting the $\partial \mathcal{P}_1(r,t)/\partial t$ term, an approximated "3-dimensional" telegrapher's equation is obtained.

[47] J. Smoller, *Shock Waves and Reaction-Diffusion Equations*, Vol. 258 (Springer, New York, 2012).

[48] M. A. Burschka, C. R. Doering, and D. ben-Avraham, Transition in the relaxation dynamics of a reversible diffusion-limited reaction, Phys. Rev. Lett. **63**, 700 (1989).